Molecular Vibration Spectra by Inelastic Electron Tunneling

J. LAMBE AND R. C. JAKLEVIC
Scientific Laboratory, Ford Motor Company, Dearborn, Michigan
(Received 1 August 1967)

An experimental and theoretical study has been carried out on the process of inelastic tunneling between metal films. The experimental results show that this process gives rise to the observation of vibrational spectra for molecules contained in the junction region. The phenomena have been studied for a number of molecular species and at temperatures ranging from 1 to 300°K. The principal effect of temperature is to broaden the observed spectral lines which can be accounted for quantitatively by considering the thermal smearing of the electron distribution in metals. Two detailed interaction mechanisms are discussed which can give rise to infrared dipole or Raman selection rules. None of the experiments carried out thus far can distinguish between these two processes, because of the low symmetry of the molecules used. In addition to the vibrational spectra, it appears that it should be possible to observe electronic transitions as well.

I. INTRODUCTION

DURING the past several years a considerable amount of experimentation has been devoted to the study of electron tunneling between metals separated by a thin oxide barrier. These have been used to study the tunneling density of states of superconductors[1] and the tunneling of supercurrents through oxide barriers,[2] as well as the nature of the tunneling barrier itself.

It has been observed recently[3] in experiments on tunneling between metals that a considerable amount of structure is observed in the voltage range 0–1 V. The structure is found to be a tunneling spectrum representing the vibrational excitation corresponding to the type of molecular species present in the barrier. The purpose of this paper is to detail further these experimental observations and report other observations which relate to the mechanisms involved in this interaction. We will discuss these experiments in terms of what we call inelastic tunneling to distinguish from the case where an electron goes through the barrier without energy loss. Inelastic tunneling results in the transfer of energy from electrons to the vibrational states of molecular species contained within the barrier.

These experiments can be understood in terms of a simple model in which the height of the potential barrier is modified by molecular species in such a way as to couple electrons to molecular vibrations. Scalapino and Marcus[4] have shown that one type of coupling leads to the usual infrared dipole selection rules. In addition, their calculation accounts for the size of the effect. Another sizable interaction which we will discuss is attributed to polarizability of the molecules and yields Raman-like selection rules.

Experimentally, several examples of tunneling spectra obtained from junctions deliberately doped with molecular impurities will be presented and discussed in relation to their support of the physical model. Tunneling spectroscopy is found to be quite sensitive, requiring only monolayer coverages to produce an easily detectable signal. We will also describe in some detail the experimental procedures.

In addition to the physics of this process, there is an aspect which relates to its use as a spectrometer. In this case, considerations such as resolution and useful spectral range are important and will be discussed.

II. THEORETICAL CONSIDERATIONS

A. Interaction Mechanisms

The process we call inelastic tunneling can be visualized in terms of a rather simple physical picture. Figure 1 represents a tunneling-junction energy-level diagram where the two Fermi levels of the metals are separated by the energy eV with V the applied voltage. According to energy conservation, the electrons in metal 1 are capable of making (elastic) horizontal transitions into empty states in the right-hand metal, provided a voltage

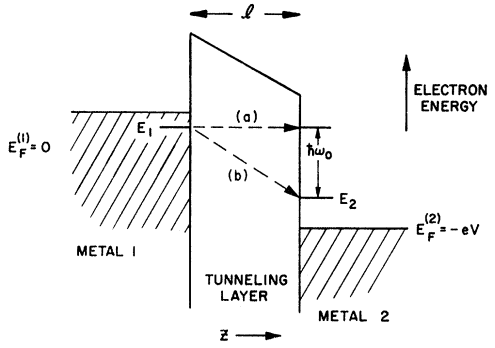

FIG. 1. Schematic energy-level diagram for tunneling between normal metals. Elastic processes (a) give rise to ordinary tunneling. In the inelastic case (b) the electron loses energy $\hbar\omega_0$ to excitation of an oscillator in the barrier region. This can only occur if $eV \gtrsim eV_0 = \hbar\omega_0$ where V_0 is the threshold voltage. The Fermi energies in the two metals are related by $E_F^{(1)} - E_F^{(2)} = eV$.

[1] Ivar Giaever and Karl Megerle, Phys. Rev. **122**, 1101 (1961); J. Bardeen, L. N. Cooper, and J. R. Schrieffer, *ibid.* **108**, 1175 (1957).
[2] B. D. Josephson, Phys. Letters **1**, 251 (1962); P. W. Anderson and J. M. Rowell, Phys. Rev. Letters **10**, 230 (1963).
[3] R. C. Jaklevic and J. Lambe, Phys. Rev. Letters **17**, 1139 (1966).
[4] D. J. Scalapino and S. M. Marcus, Phys. Rev. Letters **18**, 459 (1967).

V is applied to the junction. To a first approximation, the current-voltage characteristic of this elastic tunneling is linear. However, if it is possible for a new transfer mechanism to exist whereby an electron can tunnel from left to right and at the same time give energy to a local impurity state, a new channel for tunneling would open up. This new contribution can only occur if any empty state on the right is open for the tunneling electron, i.e., if (in the low-temperature limit) $eV \geq \hbar\omega_0$, where $\hbar\omega_0$ is the excitation energy of the impurity center. As V increases still further, current from this new process will continue to increase since more and more candidates for inelastic tunneling are brought into play. At the temperatures and excitation energies of interest, we may assume that all of the impurities are in their ground state—therefore, backward inelastic processes from right to left, or energy increasing (anti-Stokes) processes will not be significant. The onset of a new tunneling process causes an increase in the conductance at the voltage $eV_0 \approx \hbar\omega_0$ which, plotted as d^2I/dV^2, would be a peak. The line shape will depend on the natural line shape of the excitation, the temperature broadening due to the thermal smearing of the Fermi surface of the metals, and density-of-states effects in the case of superconductors. These effects will be discussed below.

The mechanism whereby coupling occurs between tunneling electrons and molecular vibrations can be thought of in terms of a perturbation of the barrier height. This can occur in a variety of ways, but here we will discuss two mechanisms which can produce such effects. These mechanisms give rise to electric-dipole or Raman selection rules in the electron tunneling spectra. Consider the situation where a small perturbing potential $U_{\text{int}}(z)$ is added to the static barrier potential $U(z)$. Harrison[5] has shown that the electronic part of the tunneling matrix element for transfer of electrons from metal 1 to metal 2 is given by

$$|M_{1,2}| \propto \exp\left\{-\int_0^l dz\left(\frac{2m}{\hbar^2}\right)^{1/2} \times [U(z)+U_{\text{int}}(z)-(E-E_1)]^{1/2}\right\}. \quad (1)$$

E is the total electron energy, z is the distance through the barrier, and E_1 is the kinetic energy associated with the component of motion parallel with the barrier. Physically U_{int} represents the actual interaction energy between the electron and a molecule in the junction. This approach was used by Scalapino and Marcus to calculate the inelastic tunneling based on the assumption that

$$U_{\text{int}} = 2ep_z z/(z^2+r_1^2)^{3/2}, \quad (2)$$

[5] Walter A. Harrison, Phys. Rev. 123, 85 (1961).

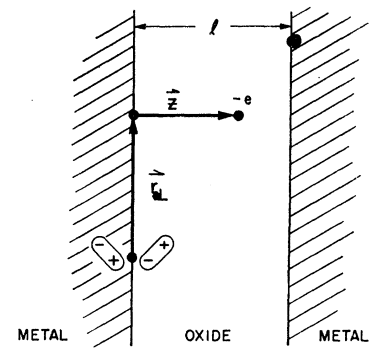

FIG. 2. Schematic showing the coordinates used to determine interaction energies of a tunneling electron and a molecule positioned near an oxide-metal interface.

where r_1 is defined by Fig. 2. They considered the case where the molecule of dipole moment p_z is located very near one of the metal electrodes so that the image dipole must be included. This yields an effective dipole $2p_z$ in the z direction. They approximated the energy $U-(E-E_1) \approx \Phi$, where Φ is the maximum barrier height, which is assumed constant. Then on expanding in powers of U_{int}/Φ,

$$|M_{1,2}| \propto \left[\left(\frac{2m}{\Phi}\right)^{1/2} \frac{ep_z}{\hbar l} g\left(\frac{r_1}{l}\right)+1\right] e^{-(2m\Phi/\hbar^2)^{1/2} l}, \quad (3)$$

$$g(x) = 1/x - 1/(1+x^2)^{1/2},$$

where the second term will give rise to the elastic tunneling current while the first represents the inelastic contribution. The use of the form of Eq. (1) involves the assumption that it is possible to ignore the fact that the final-electron-state energy is significantly different from the initial state. This is not expected to affect the physically important results. The relative magnitudes of the expected tunneling current from the two mechanisms discussed below should be of significance.

Consider a simple molecule with a single vibrational frequency ω_0. The complete matrix element $\langle 1\|M_{1,2}\|0\rangle$ is then between the ground state and first excited vibrational state, and represents the tunneling of a single electron which gives up energy $\hbar\omega_0$ to the vibration in the process. This assumes, of course, that the dipole moment p_z of the molecule is a function of the normal coordinate of the vibrator. Such vibrational states are termed infrared active. The current flow contributed by these inelastic processes is then obtained by summing transition rates over the occupied states on the left and the empty ones on the right.[4,5] We have the additional condition for conservation of energy which requires $E_1+eV = E_2+eV_0$.

The actual calculation follows use of the golden rule

and gives[6]

$$I_i(\omega_0,V)=\left(\frac{dj}{dV}\right)_0|\langle 1|p_z|0\rangle|^2\left[\frac{4\pi me}{\hbar^2\Phi}\right]\times\ln\left|\frac{l}{r_0}\right|\int_{-\infty}^{\infty}dE\,f(E)[1-f(E+eV-\hbar\omega_0)]\times N_1(E)N_2(E+eV-\hbar\omega_0),\quad(4)$$

where $N_1(E_1)$ and $N_2(E_2)$ are effective tunneling density of states which for normal metals are equal to unity. $(dj/dV)_0$ is the normal junction elastic conductance per unit area, $f(E)$ is the Fermi function, and $|\langle 1|p_z|0\rangle|^2$ is the dipole matrix element for the vibrational transition. A term $2\pi l^2\ln|l/r_0|$ results from the integration of $g(r_1/l)$ over an area extending from a radius r_0 to a radius l, where r_0 is the cutoff distance in the vicinity of the molecule. For $r_1>l$, g^2 is small. This represents an effective cross section for tunneling. The simplifying assumption has been made that the electronic barrier penetration probability is constant with electron energy.

This form will be useful for discussing instrumental linewidth for a single vibrational excitation of energy $\hbar\omega_0$. In any real case, however, we must consider a distribution of oscillator frequencies to represent the real excitation spectrum. This amounts to summing the above expression for I_i over the spectrum. In doing this the total inelastic current due to N molecules will be

$$I_i(V)=N\left(\frac{dj}{dV}\right)_0\left[\frac{4\pi me}{\hbar^2\Phi}\right]\ln\left|\frac{l}{r_0}\right|\sum_m|\langle m|p_z|0\rangle|^2\times\int_{-\infty}^{\infty}dE\{f(E)[1-f(E+eV-\hbar\omega_m)]\}\times N_1(E)N_2(E+eV-\hbar\omega_m),\quad(5)$$

where N is the total number of oscillators and $\langle m|p_z|0\rangle$ is the dipole strength of the individual oscillators. It is useful to evaluate d^2I/dV^2 and dI/dV in the low-temperature limit and one obtains

$$d^2I/dV^2=N\left(\frac{dj}{dV}\right)_0\left[\frac{4\pi me}{\hbar^2\Phi}\right]\times\ln\left|\frac{l}{r_0}\right|\sum_m|\langle m|p_z|0\rangle|^2\delta(eV-\hbar\omega_m),\quad(6a)$$

$$dI/dV=N\left(\frac{dj}{dV}\right)_0\left[\frac{4\pi me^2}{\hbar^2\Phi}\right]\times\ln\left|\frac{l}{r_0}\right|\sum_m|\langle m|p_z|0\rangle|^2S_m(eV),\quad(6b)$$

where S_m represents a unit step at $eV=\hbar\omega_m$. This means that the second derivative yields directly the infrared absorption spectrum $\sum_m|\langle m|p_z|0\rangle|^2\delta(eV-\hbar\omega_m)$. The above expression (6b) was used by Scalapino and Marcus to estimate the size of such effects for a coverage of one molecule per 10 Å^2. A reasonable value for $\sum_m|\langle m|p_z|0\rangle|^2$ is 10^{-38} esu^2 cm^2. They found that there would be about 1% increase in conductance.[4]

The foregoing is a review of the calculation of Scalapino and Marcus[4] for the case of infrared active modes. The calculation will now be extended to the Raman type of interaction. It is important to notice that there are other mechanisms by which an electron can interact with a localized molecular impurity. Of direct importance to the present experiments is the interaction through the polarizability of the molecule. Though a given molecule may not have a dipole moment associated with a given vibrational mode, there will usually be a polarizability associated with the mode.[7] Since the electric field at the molecule due to the tunneling electron and its image are of the order of 10^6–10^7 V/cm, it will be seen that the interaction energy of the electron with the induced dipole moment is significant. This interaction energy, taking into account the nearest images of the dipole and electron, is

$$U_{\rm int}(\alpha)=-4e^2\alpha z^2/(z^2+r_\perp^2)^3.\quad(7)$$

This energy can be used within the same approximation of Ref. 4 to compute the matrix element for the inelastic contribution to the tunneling current. This is

$$|M|\propto\left[\left(\frac{2m}{\Phi}\right)^{1/2}\frac{1}{\hbar}\frac{\alpha e^2}{4l^3}t\left(\frac{r_\perp}{l}\right)+1\right]e^{-(2m\Phi/\hbar^2)^{1/2}l},\quad(8)$$

which is to be compared with Eq. (3). The function

$$t(x)=\frac{1}{x^2}\left[\frac{1-x^2}{(1+x^2)^2}+\frac{1}{x}\tan^{-1}\left(\frac{1}{x}\right)\right]$$

contributes little for $r_1>l$ and can be estimated numerically. The inelastic current will now be given by

$$I=N\left(\frac{dj}{dV}\right)_0\left[\frac{4\pi m}{\hbar^2\Phi}\frac{e^3}{16l^6}\right]\left[\int_{r_0}^{l}t^2r_\perp dr_\perp\right]\sum_m|\langle m|\alpha|0\rangle|^2\times\int_{-\infty}^{\infty}dE[f(E)(1-f(E+eV-\hbar\omega_m))]\times N_1(E)N_2(E+eV-\hbar\omega_m),\quad(9)$$

where $\langle m|\alpha|0\rangle$ is the appropriate matrix element of the polarizability which has been assumed a scalar, although in general it is a tensor quantity. For typical Raman-active vibration lines $\sum_m\langle\alpha\rangle^2\simeq10^{-50}$ cm^{-6}. Direct comparison of the conductance change due to this case with that estimated above for the dipole

[6] The factor $[f(E_1)-f(E_2)]$ was used in Ref. 4 instead of the correct form $f(E_1)[1-f(E_2)]$. This, however, does not affect the validity of the low-temperature results obtained there.

[7] Gerhard Herzberg, *Infrared and Raman Spectra of Polyatomic Molecules* (D. Van Nostrand Co., Inc., New York, 1945).

transitions show them to be of nearly the same order of magnitude although the Raman-active transitions are expected to be the weaker of the two when the dielectric constant of the oxide is taken into account. Therefore one can expect that both Raman-active as well as infrared-active vibration modes should be observed in inelastic tunneling spectra. So far, the molecules studied experimentally have such low symmetry that all normal modes are expected to be both infrared (IR) and Raman active.

B. Spectral Linewidths

Independent of the details of the interaction mechanisms discussed, some comments on expected linewidths for these experiments can be made. Consider a single sharp transition for a molecule located in the junction. To compute the linewidth, the essential thing to consider is the onset of inelastic tunneling as the voltage between two metals gradually approaches and passes through the threshold region.

First consider the case where both electrodes are normal metals as illustrated in Fig. 1. The electron in metal 1 goes into metal 2 and loses energy $\hbar\omega_0=eV_0$. Under these conditions we wish to examine the terms which relate to the instrumental linewidth which will be observed in the second derivative curve. For this purpose note that the voltage dependence of Eq. (4) is contained in the Fermi functions for the two normal metals and $N_1(E_1)$ and $N_2(E_2)$ are set equal to unity. Thus we need only consider the integral involving the term $f(E)[1-f(E+eV-eV_0)]$, which is

$$I_i=C\int_{-\infty}^{\infty}dE\left(\frac{1}{1+e^{E/kT}}\right)\left(1-\frac{1}{1+e^{[E+e(V-V_0)]/kT}}\right), \quad (10)$$

where C takes into account all the various tunneling parameters which are independent of E and T within the assumptions. This yields

$$I_i=Ce(V-V_0)\frac{e^{e(V-V_0)/kT}}{e^{e(V-V_0)/kT}-1} \quad (11)$$

giving I_i as a function of the difference voltage $(V-V_0)$. Taking derivatives,

$$\frac{d^2I_i}{dV^2}=C\frac{e^2}{kT}\left[e^v\frac{(v-2)e^v+(v+2)}{(e^v-1)^3}\right], \quad (12)$$

where

$$v\equiv\frac{e(V-V_0)}{kT}.$$

This describes the line expected for an extremely narrow vibrational excitation in which case the observed linewidth will be due entirely to the smearing in energy of the electron distribution in the metals. The above functions are plotted in Fig. 3. Note that the half-width is given by $5.4kT$. This thermal broadening is a rather

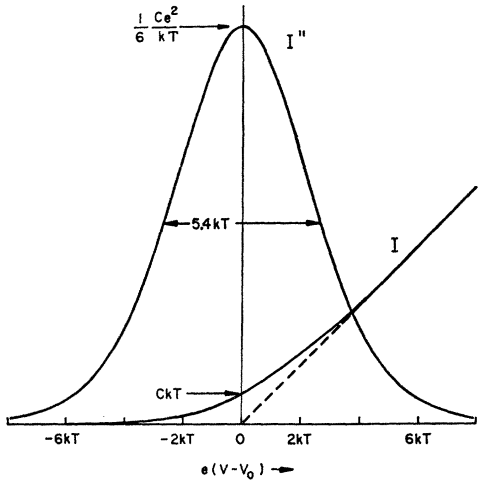

FIG. 3. Inelastic tunneling current between normal metals as predicted by Eq. (11) and its second derivative from Eq. (12). The predicted linewidth at half maximum is $5.4kT$. The abcissa, which represents the applied voltage, is plotted in units of kT. The intercepts on the vertical axis are as indicated. The slope of the dashed line is the asymptotic conductance for $eV\gg\hbar\omega_0$.

fundamental property of the inelastic tunneling. Of course there will be other sources of broadening in the actual vibrational levels. Nevertheless there is a lower limit on the instrumental linewidth which places an ultimate limit on the resolving power of a tunneling spectrometer when using normal metals.

In the case of superconducting electrodes the situation is different since now we must consider the changes in tunneling density of states. Consider the case of two superconducting (Fig. 4) electrodes of gap 2Δ and temperatures where 2Δ is large compared to kT. As before, energy conservation requires

$$eV+E_1=eV_0+E_2.$$

Now, however, the function $f(E_1)[1-f(E_2)]$ is equal to

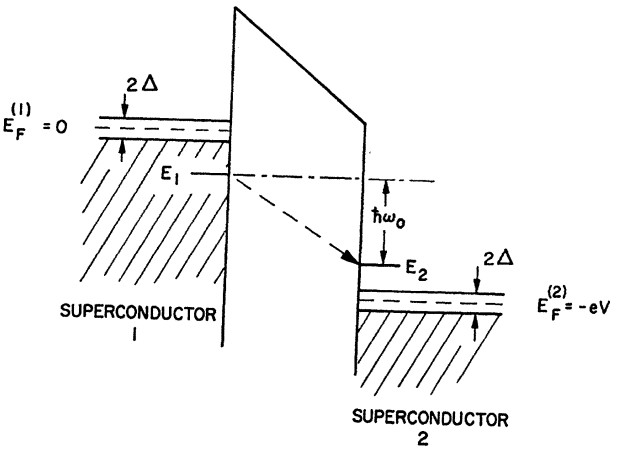

FIG. 4. Energy-level schematic for tunneling between superconductors. The energy gap of width 2Δ represents forbidden states for tunneling.

unity since $2\Delta \gg kT$ so the appropriate integral to be examined is given by

$$I_i = C\int_0^\infty N_1(E)N_2(E+e[V-V_0])dE. \quad (13)$$

The superconducting density of states has an energy gap 2Δ symmetrical about the Fermi level and is sharply peaked near the gap edges.[1] The presence of the gap and sharply peaked density of states both act to increase the resolution of an inelastic tunneling threshold. The current will follow just the usual I-V curves found for elastic tunneling between superconductors, but displaced by V_0. Note that the onset of inelastic tunneling is displaced upward by 2Δ from eV_0 due to the gap. That this should occur is easily seen from Fig. 5, where we see clearly that $V > V_0$ at threshold. Also note the line shape is different in that a shallow dip appears at the trailing edge. We shall define the linewidth in terms of the sharp peak. The important point here is that the instrumental linewidth for this case is defined as that measured in the usual superconducting tunneling experiment. Rather than examining Eq. (13) theoretically, it is useful to compare it with the experimentally observed tunneling current between superconductors. Tunneling experiments show that the sharp peak in tunneling density of states is rounded off compared to the ideal BCS prediction, and this results in smearing of the threshold. Comparison with a current-voltage curve taken from experimental parameters is shown in Fig. 5. As an example we note that Giaever[8] *et al.* have measured this for an Sn-SnO_2-Sn junction and gives a value of $\delta = 0.03$. This yields a linewidth of about 30 μV or 0.25 cm^{-1} as the limiting resolution at low temperatures. At the temperature at which this measurement was made, 0.3°K, the theoretical linewidth using normal electrodes would be 150 μV. Thus superconductors should improve resolving power over that obtained for normal metals.

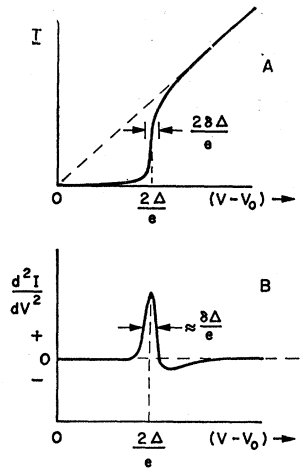

FIG. 5. Curves representing inelastic tunneling for the case of two superconductors. (A) represents the I-V curve near the onset of inelastic tunneling. The second derivative shape is indicated in (B). Effective linewidth is determined by the width δ which is characteristic of the onset of tunneling. The line position is $eV_0+2\Delta$.

III. EXPERIMENTAL TECHNIQUES

A. Sample Preparation

1. Films

The tunneling junctions were of the usual metal film–insulating oxide–metal-film structure and with few exceptions these were Al-Al_2O_3-Pb. Preparation was done in bell-jar–type vacuum chambers. Two types of vacuum systems were used. The first was an oil-diffusion–pumped ($\simeq 10^{-7}$ Torr) system with liquid-nitrogen trapping and a zeolite trap on the foreline. The other was an ion-pumped oil-free system ($\simeq 10^{-9}$ Torr ultimate). Both systems used Viton gasket seals and could be given a moderate degassing by heating to 100°C by internal operation of a filament. All fixtures were either of stainless steel, copper, Al, Teflon, or ceramic. Both systems were equipped with a gas-discharge electrode made of aluminum which could be operated with O_2 gas immediately after initial pump-down to promote cleanup of residual impurities. This discharge was also used for promoting oxide growth later in the process.

Sample substrates were of fused silica of dimension $\frac{1}{2}\times 1\frac{1}{2}$ in.$\times 1$ mm with prefired silver paste electrodes. They were first scrubbed in detergent, rinsed in deionized water for $\frac{1}{2}$ h or more and finally dried in propyl alcohol vapor. The samples were then mounted in the vacuum chamber in a rotatable mask changer which allowed the entire fabrication to take place without exposure to atmosphere. The mask provided for initial evaporation of an aluminum strip 1–2 mm wide ($\sim$2000 Å thickness) the length of the substrate. Masks could then be moved aside for oxidation of the Al. Three Pb films were then evaporated crosswise to form junctions 1×1 mm^2. This area was found to be large enough for easy masking, and yet it produced a high yield of defect-free samples. The area was large enough so that, with the impedances used ($\approx 100\,\Omega$), current densities were not so high as to cause serious breakdown and noise problems.

2. Oxidation

Oxidation of the aluminum film was done by one of two methods. In the first, the sample was removed from the vacuum system and exposed to room air for 18–24 h. The edges of the aluminum film in this case were usually masked by painting over the edges with Formvar paint after it was suspected that shorts and other defects occurred there. This method suffers from unavoidable contamination of the junction by organic impurities

[8] I. Giaever, H. R. Hart, Jr., and K. Megerle, Phys. Rev. **126**, 941 (1962).

from both the paint and the atmosphere. On the other hand, it was found that simple exposure of the aluminum to pure oxygen at temperatures as high as 200°C would not result in appreciable tunneling oxide layers. In this case, resistances of less than 0.1 Ω were obtained, which indicated oxides <10 Å thickness. In such cases, the junctions showed a good Josephson effect when both metals were superconducting. Water and organic films are probably responsible for the thicker insulators (≈30 Å) formed by exposure to air.

Therefore, the gas-discharge oxidation technique described by Miles and Smith[9] was used. An electrical discharge was set up between an aluminum cathode at −500 V dc and the rest of the system while maintaining a pressure of approximately 50×10^{-3} Torr of either high-purity or standard tank oxygen. Care was taken to keep the aluminum electrode close enough (3 in.) for efficient oxidation and yet remain shielded from a direct optical path to the samples. Without shielding the results were very erratic. Exposure of the samples to the discharge for 20 min or more produced a 10–20-Å insulator. A small dc oxidizing potential (1 V) applied to the Al films promotes slightly thicker oxide growth closer to 30 Å. Samples prepared this way showed no organic contamination. When following this procedure, no significant differences were found between use of either type of vacuum system. Apparently, with proper trapping, contamination from pump oil is not appreciable. As will be seen, we have not been successful in eliminating effects caused by water vapor, present either as residuals in the chamber or as water liberated from the system walls during operation of the discharge.

3. *Molecular Additions*

Deliberate doping of junctions by impurities was done by exposing the Al oxide surface to a vapor of the substance to be deposited. For the case of the liquids (acetic and propionic acids and methyl and ethyl alcohols, water), a drop or two was sealed in a small capillary and broken inside the vacuum chamber after oxidation. A resistance heater was provided to aid evaporation of less volatile materials (cyanoacetic acid). The pressure quickly rose to 10^{-2}–10^{-1} Torr as measured by a thermocouple gauge with subsequent slow decrease due to adsorption of the vapor on the chamber surfaces and sample. After 5–10 min exposure, the system is again evacuated and the top Pb film deposited. For the case of the hydrocarbon (Convoil 20 pump oil), its vapor pressure was low enough simply to place a tiny amount (10^{-4} g) in a tantalum boat approximately 10 in. from the sample and to evaporate the material at the appropriate time by heating slowly to several hundred degrees centigrade. In each case it is estimated that approximately one monolayer or less is deposited. This estimate is based on the measured pressure drop after initial exposure or actual amount evaporated, in the case of pump oil. In particular, the acids are known to adsorb to a single monolayer. None of the organics used presented a contamination problem and could be successfully purged from the system with a draft of warm air and routine pumping. Although the majority of junctions were Al-Al_2O_3-Pb combinations, a number of metals were successfully used. Au, Sn, Al, Mg and Cr in place of the Pb all showed inelastic tunneling as did the combination Ta–Ta oxide–Pb.

Junctions made according to the outlined procedure had nominal tunneling resistances of 30 Ω to 30 kΩ, although the most convenient resistances were in the 30–200 Ω range. Usually, for the doped samples, several attempts were necessary before the right combination of time of exposure to anodization and organic vapor was achieved. Experience indicates that the presence of the organic layer increases the resistance of the tunnel junction, in some cases amounting to an equivalent Al oxide dielectric thickness of about 10–20 Å. It was usually necessary to decrease the amount of oxidation to accommodate the presence of the organic film and obtain a workable junction resistance. All of the samples were reasonably stable for a period of hours up to one day. However, those doped with organics were more unstable and tended to deteriorate with the resistance dropping and becoming noisy over a period of weeks, probably because of decomposition or reaction of the organics. The pure oxide junctions were the most stable structures, and showed slow increase of resistance with time.

The organic materials employed so far were either of the type which form strong adsorbing bonds (acids, alcohols) or were of high enough molecular weight so that the adsorbed layer was stable. However, some materials (e.g., acetone, benzene, chloroform) were found not to adsorb on the Al-Al_2O_3 surface in sufficient quantity to produce detectable spectra. These, and others like them, could probably be adsorbed by first cooling the samples as low as liquid nitrogen temperatures (77°K). After the proper exposure to organic vapor, the top metal film could be deposited. This was not done in the present experiments.

B. Measurements Technique

The measurement which one wishes to make is essentially a careful study of the current-voltage relationship of a tunnel structure. It is well known that this can be done in a very sensitive way by using derivative techniques.[10] We therefore used the method of harmonic generation to measure the second derivative of the *I-V* curve. The essence of this method is to detect changes in conductivity by detecting the generation of second harmonic where the *I-V* curve is nonlinear. The circuit used yields an ac signal voltage whose amplitude is

[9] J. Miles and P. Smith, J. Electrochem. Soc. **110**, 1240 (1963).

[10] William R. Patterson and J. Shewchun, Rev. Sci. Instr. **35**, 1704 (1964); D. E. Thomas and J. M. Rowell, *ibid.* **36**, 1301 (1965).

proportional to the second derivative of current with respect to voltage. The proportionality factor contains the junction impedance as a factor, but this did not vary greatly over the ranges studied. A schematic of the apparatus is shown in Fig. 6.

We chose a primary frequency of 50 kHz and detected at 100 kHz. This frequency was used to minimize any excess noise from the sample and because the amplifiers used had optimum noise figure in this frequency range. We have not made any detailed study of the excess noise from our tunnel junctions, but it did appear that such noise dropped off with frequency. The large capacitance effects of the junction made it inconvenient to go to much higher frequencies to study this over a wide range.

The sample resistance plays an important role in determining the over-all sensitivity of such systems. The lower the sample resistance, the greater the available signal power. It is desirable, therefore, to have the sample impedance as low as possible consistent with required breakdown strength. In our case this impedance was about 100 Ω for a mm² sample. A transformer is used to optimize the input impedance to the preamplifier.

In the discussing the measurements we will refer to these second derivative curves as spectra. It will be noted, in fact, that the curves resemble very closely conventional infrared absorption spectra. Thus the data is obtained in a very convenient form. The reason for this was seen in detail in the sections on linewidths and mechanisms. Suffice to say that the second derivative curves can conveniently be thought of in terms of absorption lines. Thus, for example, to compare the relative over-all strength of two inelastic processes, one would compare the areas under the appropriate second derivative curve.

The amplitude of 50-kHz modulation which can be used is determined by the linewidths to be resolved. Thus for most of the spectra reported here modulations of between 1 and 5 mV were employed. The smaller modulation results in smaller signal, of course, but its use was necessary to assure optimum resolution in some cases.

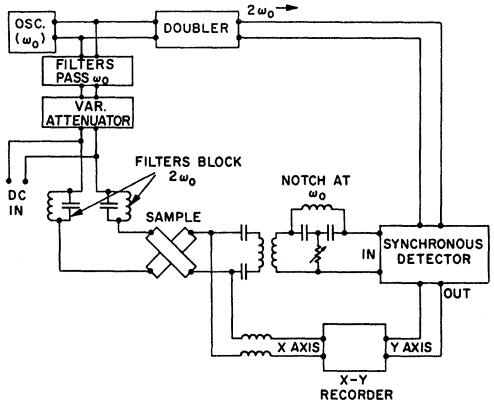

FIG. 6. Schematic of circuitry for taking second derivative d^2I/dV^2.

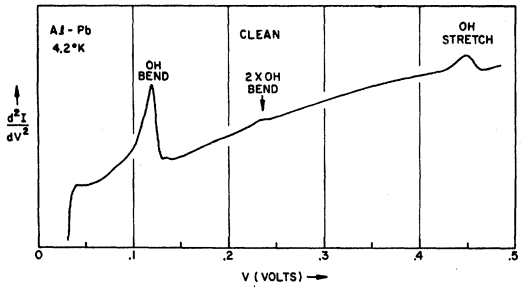

FIG. 7. Tunneling spectrum from Al-Pb junction prepared without organic impurities. The peaks at 120 mV and 450 mV are the bending and stretching vibrations respectively of OH present in the oxide. Also the first overtone of the OH stretch is visible at 240 mV.

Conventional cryogenic techniques were employed. Sample slides were mounted on a rod containing stainless steel outer conductor and copper inner conductor coaxial leads. They were then immersed directly in the liquid refrigerant (liquid helium, liquid nitrogen, or dry ice and acetone) in order to take spectra at various temperatures. Temperatures as low as 0.9°K were attainable by pumping on the helium bath. The entire Dewar was shielded with a μ-metal cylinder.

IV. EXPERIMENTAL RESULTS

A. Tunneling Spectra

A number of tunneling spectra have been obtained from clean junctions as well as from those in which various impurities were deliberately introduced. The latter spectra include the introduction of heavy water, organic impurities introduced simply by exposure to the atmosphere, and the introduction of known compounds. The known compounds include a pure hydrocarbon, acetic and propionic acid (and their deuterated forms), cyanoacetic acid, ethyl and methyl alcohol, and water (and heavy water).

It should be possible to explain all the details of the tunneling spectra in terms of details of molecular structure together with possible perturbations due to adsorption. This has not been attempted in the present studies. Only a general interpretation of the various spectra will be given and the energy of observed bands will be identified with the help of IR data, when available.[11] Sufficient analysis is done to present a convincing argument concerning the validity of the basic interpretations.

1. Clean Junction

The data in Fig. 7 show the results obtained for an Al-Al_2O_3-Pb junction whose oxide was prepared in a pure oxygen discharge. The features of this clean

[11] *Sadtler Standard Spectra* (Sadtler Research Laboratories, Philadelphia, Pa.).

spectra are two large peaks at 120 and 450 mV. These peaks can be associated with the bending and stretching modes of OH groups. The first harmonic line of the bending frequency is also seen. This means, of course, that OH was introduced during the process of forming the oxide or adsorbed on the oxide surface before the second electrode was deposited. We have not been able to eliminate this effect. The background was the same for the ultrahigh-vacuum samples as for a well-trapped oil diffusion system. Thus it appears that the attempts to produce a clean junction (i.e., pure aluminum oxide) were not completely successful in that OH was still present. We note, however, that the insulator could be made essentially free of any organic molecules. This result was true for the nonbaked ion-pumped system as well as for the nitrogen-trapped oil diffusion system.

One might also expect to see the Al_2O_3 vibrational spectrum in the region below 100 mV. Since most of the junctions had at least one superconducting electrode, the large phonon spectra associated with the Pb density of states became prominent and masked any smaller structure. However, a number of Al-Al_2O_3-Al junctions were studied at low voltages at 4.2°K, presumably well above the transition temperature. There is a peak at 35 mV of about $\frac{1}{10}$ the intensity of the OH lines and some indication of a small broad peak at 60 mV. However, we do not positively identify these with Al_2O_3. Indeed it must be considered a possibility that these peaks are to be associated with the Al metal phonons. Aluminum would be expected to have a phonon peak in the 35-mV region.[12] Structure symmetrical about zero voltage was also seen in these Al-Al_2O_3-Al junctions corresponding to a resistance maximum about 2 mV wide. Its strength was approximately $\frac{1}{10}$ that of the OH vibrational bands.

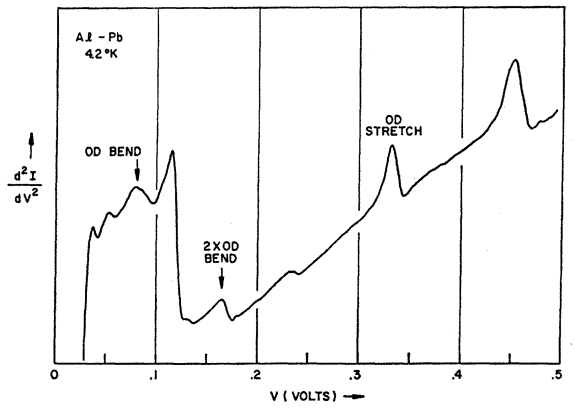

FIG. 8. Tunneling spectrum of Al-Pb junction in which the oxide was formed in the presence of D_2O. In addition to the lines in Fig. 7, there are now the OD bending and stretching lines at 80 mV and 330 mV, respectively. The overtone OD bending line is also present.

[12] J. L. Yarnell, J. L. Warren and S. H. Koenig, in *International Conference on Lattice Dynamics, Copenhagen, 1963*, edited by R. F. Wallis (Pergamon Press, Inc., New York, 1965).

2. Heavy Water

In order to be more certain of the interpretation of of the foregoing effects, experiments were carried out with the addition of D_2O to the oxide. This was done in two ways. The first method was to add D_2O to the oxygen being used in the discharge. The partial pressure of D_2O was $\approx 20\times10^{-3}$ Torr with 60×10^{-3} Torr O_2. The second method was to expose the oxide to D_2O vapor after the oxide had been formed in the discharge. In both cases, structure due to the OD bond vibration was found. This resulted in spectra shown in Fig. 8. The OD bending and stretching vibrations are shifted down in energy by the factor of approximately $(\sqrt{2})^{-1}$ as expected. The largest signals were obtained for the samples which were made with the D_2O in the oxygen discharge. Also the first harmonics of the OH and OD bending modes are easily detected.

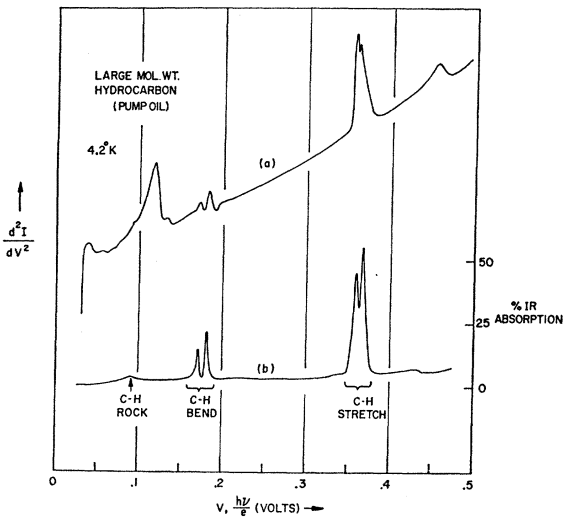

FIG. 9. Tunneling spectrum (a) with a monolayer of large molecular weight hydrocarbon. For comparison an IR absorption spectra (b) of the same material is also shown. In addition to the OH lines, the principal hydrocarbon vibrations appear at about 360 mV, 175 mV, and 90 mV which are the CH stretching, bending, and rocking modes, respectively.

3. Hydrocarbons

Figure 9 shows the tunneling spectrum of a sample of hydrocarbon oil (Convoil-20). This system is expected to be simple in the sense that no strong chemical reaction is expected between the oil molecules and their surroundings inside the junction. At any rate, the tunneling spectrum is quite simple, showing only four strong lines caused by the hydrocarbons. These CH modes are the stretching mode at 360 mV, two bending modes near 175 mV and the rocking mode at 90 mV. Also shown, on the same voltage scale, is the IR absorption spectra of the oil. The strong absorption lines appear at values of energy very close to the tunneling

bands. This close agreement is expected of the CH frequencies since they are known to be relatively insensitive to changes in surroundings and differ little from one compound to another. In particular, the CH stretch band is especially prominent in and distinctive of most organic materials. Also indicated are the OH frequencies attributable to the nature of the oxide layers and which also could arise by reaction and oxidation of some of the hydrocarbon. The latter mechanism is inferred from the observation that when stored for periods as short as one day, these junctions showed a growing OH band in relation to the CH. The overtone frequency of the OH stretch has been observed at about 930 mV for samples which have developed a very strong OH band. This is the highest energy band observed to date. This is of special interest in connection with the useful spectral range of tunneling spectrometers.

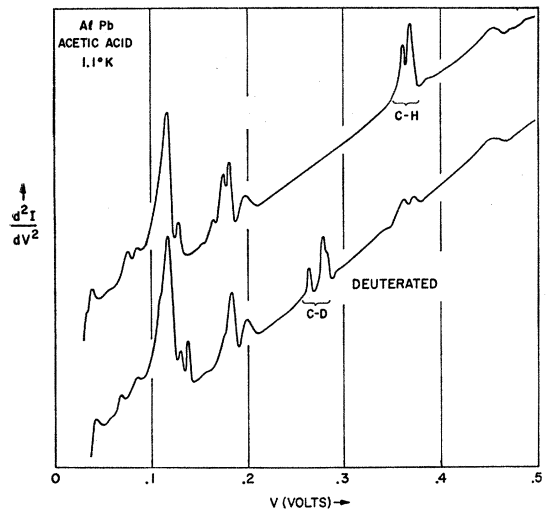

FIG. 10. Tunneling spectra of acetic acid present as one monolayer in both undeuterated CH_3COOH and deuterated CD_3COOD forms. Prominent are the CH and CD stretching bands at about 360 mV and 275 mV. The lines at lower energies are related to the other CH and CO vibrations.

4. *Organic Acids*

In Figs. 10 and 11 are shown tunneling spectra of acetic CH_3COOH and propionic $CH_3(CH_2)COOH$ acids. These were adsorbed on the Al oxide at room temperature. The spectra show the expected CH stretching lines at 360 mV and the CH deformation region below 200 mV. Of interest is the fact that the C=0 stretch, usually seen at 230 mV in IR absorption, is not present. Nearby at 200 mV is a broadened line which could be a shifted C=0 frequency. Such a large perturbation on a vibration could be expected in this case since this bond is at the acid group end of these molecules, which could be perturbed by interaction with the Al oxide, or even by direct reaction with the Pb to form lead acetate. Also shown are the tunneling

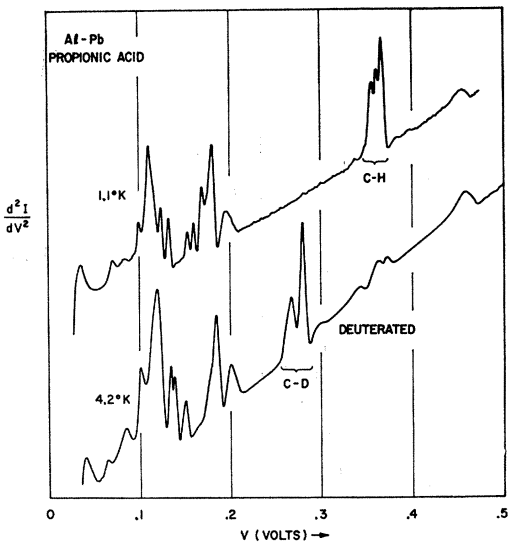

FIG. 11. Tunneling spectra of propionic acid present as one monolayer in both undeuterated CH_3CH_2COOH and deuterated CD_3CD_2COOD forms. The spectra are very similar to those for acetic acid (Fig. 10) as expected.

spectra of these same acids in their partially deuterated form. One sees immediately the appearance of the CD stretch bands in both spectra.

In Fig. 12 is shown the tunneling spectrum of cyanoacetic acid CNCOOH which, although similar in many details to the other acids, shows the C≡N stretching mode at 280 mV. This line is very sharp in most IR absorption spectra and is in a relatively vacant region of the spectrum. This sharp line was used to observe the small ($\approx$1 mV) shift in line position when the Pb is made normal.

5. *Miscellaneous*

Figure 13 shows the tunneling spectra of methyl and ethyl alcohols adsorbed at room temperature, giving results which are characteristic of alcohol gas IR spectra of these molecules.

As a last example of doped junctions, the spectrum of Fig. 14 shows the trace obtained from a junction

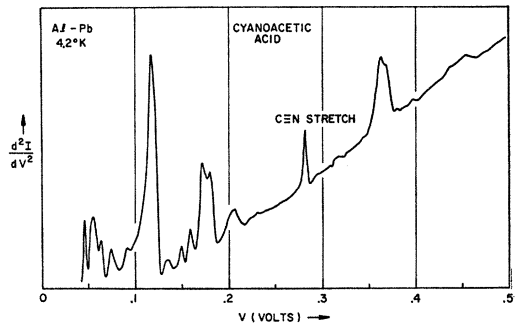

FIG. 12. Tunneling spectra of cyanoacetic acid CNCOOH. Although similar to the other acids, this spectrum has the C≡N stretching line at 280 mV.

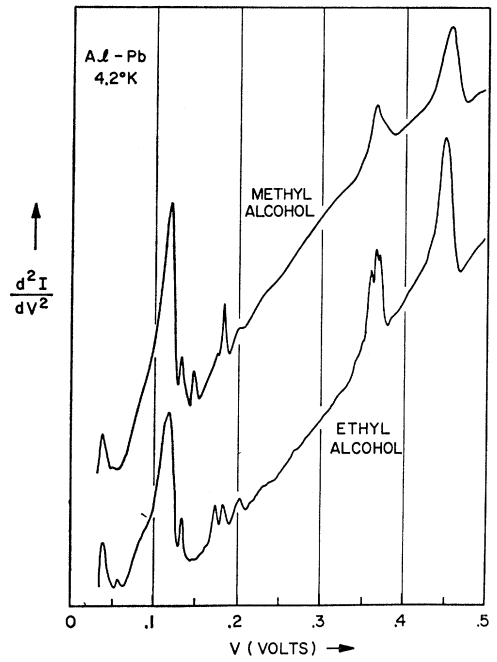

FIG. 13. Tunneling spectra of methyl and ethyl alcohol present as adsorbed monloayers.

oxidized by exposure to room air for approximately one day. This spectrum shows the appearance of what clearly are organic impurities picked up by the junction. When Formvar paint was used to mask off the edges of the Al film, a different type of spectrum was obtained which, however, was clearly indicative of contamination by an organic species. Pickup of organics from the air could be observed in the tunneling spectra with only a few minutes of exposure of a freshly made oxide to ordinary room air.

6. General Observations

In general, then, these spectra of the various organic materials show that the inelastic tunneling is in reality a new spectroscopy. The total number of molecules actually involved for the 1-mm² junction area is estimated to be of the order of 10^{12} for the case of a single monolayer. In Sec. III we indicated that a monolayer of molecular impurity was added. For the more prominent spectral lines, the conductance change is of the order of 1–2% and is still quite easily observable using an integration time of one second on the phase-sensitive detector. It is estimated that about 1/100 of a monolayer or a total of 10^{10} molecules/mm² are detecable. It should be possible to improve on the sensitivity by using longer integration times on the detector and by the use of larger junction areas. The feasibility of such steps must be explored experimentally before the question of ultimate sensitivity is fully answered.

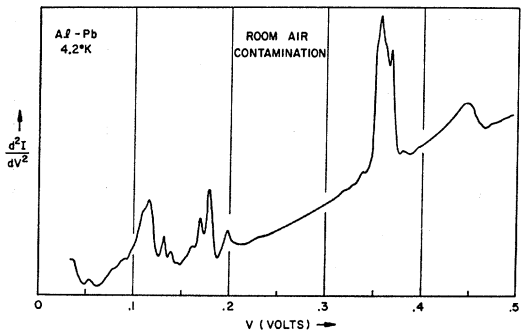

FIG. 14. Tunneling spectra of Al-Pb junction exposed to room atmosphere for 18 h. Very pronounced organic signals are seen and contamination of the order of one monolayer is estimated.

Most of the above spectra were obtained from the Al-Pb combination. However, other combinations have shown the behavior. Al-Al_2O_3-Au (acetic acid, room air), Al-Al_2O_3-Sn (room air), Al-Al_2O_3-Al (acetic, room air), Ta-(Ta oxide)-Pb (room air), Ta-(Ta oxide)-Sn (room air), and Mg-(Mg oxide)-Pb (room air) have all shown organic tunneling spectra. This is experimental support for the general occurrence of this phenomena.

Studies were made to see if the type of spectra observed depended on the polarity of the applied voltage. There is generally a built-in asymmetry in such junctions due to work function differences between the two metals. This gives rise to different conductivities in the two directions and this influences the sensitivity of the measurement somewhat. The positions of spectral lines are the same independent of the direction of the applied voltage. The normal conductance does vary somewhat over the range of voltages which we use and this effect is also asymmetric. Usually spectra were taken with the polarity such that the change in normal tunneling conductance with voltage was minimized. This corresponds to Pb positive for Al-Al_2O_3-Pb junctions.

B. Temperature Effects

The most striking temperature effect is related to the change in observed linewidth. As the temperature at which the sample is studied is increased, the lines broaden and the peak height decreases. This is illustrated by Fig. 15 which shows the CH line for a large hydrocarbon as measured at 77°K. At 4.2°K the linewidth is about 15 mV, but at 77°K the linewidth is about 40 mV. At higher temperatures the line continues to broaden and at 195°K (dry ice temperature) the line is about 90 mV wide. At room temperature the broadening is too great to get any reasonable estimate of linewidth. The peak height decreases with temperature. The intensity of the lines, however, in terms of the area under the curve appears to remain constant. This could only be checked up to 77°K with any confidence.

At the low temperatures, the Pb electrode is superconducting and this results in narrower lines. If a magnetic field is used to quench the superconductivity,

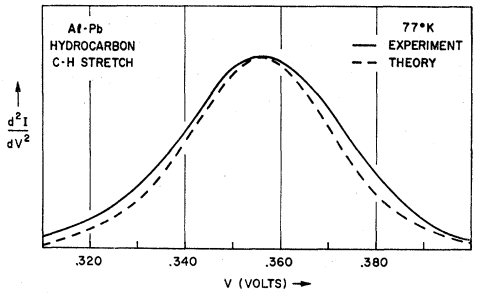

FIG. 15. Comparison of observed width of the CH stretching line to Eq. (12) at 77°K. The peaks were normalized at their maxima. The slight excess of experimental width over theory is probably due to the natural width (≈18 mV) of the line determined at 4.2°K.

a broadening of the lines occurs at 4.2°K. This is shown in Fig. 16. There should also be a slightly shift in the line peak. This shift will be of the order of 1 mV for an Al-Al_2O_3-Pb junction. Thus the shift is not readily apparent on the scale of the above figure. We therefore used the C≡N vibrational line of cyanoacetic acid (Fig. 12) to test for this shift. This is a very narrow line and so one could expect to see the slight shift as the lead and aluminum went from normal to superconducting. This measurement was carried out at 1.0°K. It was observed that when the superconductivity of the Al and Pb was quenched by a magnetic field, the line peak shifted to lower voltages by approximately 1 mV.

V. DISCUSSION

A. Spectra

The most important result is the line shift produced by deuteration. This conclusively establishes that the interactions observed are associated with molecular species included in the barrier region. Of course, the change in spectra with the use of different molecules also confirms this. It is expected that the observation of selection rules will provide insight into the details of the mechanism. The lines which we can see and identify do indeed correspond to lines that appear strongly in ordinary infrared spectra and hence are allowed dipole transitions. We have noted, however, that in all the cases studied, these transitions are also expected to be Raman active. Thus it has not yet been established firmly whether the infrared-like processes dominate, or whether both effects contribute. In order to study the selection rules, one needs to study a case where certain transitions are strongly allowed by one mechanism and very weak for the other mechanism. This requires molecules with the proper symmetry. It would also be necessary, for example, to insure that the adsorption interactions do not destroy the requisite symmetry.

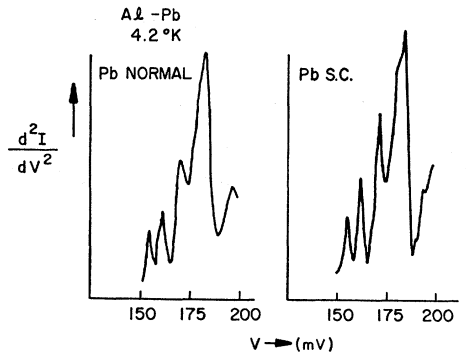

FIG. 16. Comparison of a portion of a propionic spectrum taken at 4.2°K showing the effect on resolution when both metals are normal and one (Pb) is superconducting (S.C.). The superconductivity of the lead was quenched with a magnetic field of 7500 G in order to obtain the normal-metal spectrum.

In the same vein one would hope for some evidence of orientation effects of the molecules. This is because the simple theory indicates that only the dipole component perpendicular to the metal electrode is effective. We have no definite evidence for such an effect as yet. It is worth noting that the OH vibrations should provide a nice test for this if OH can be adsorbed in different orientations. In the extreme case where OH lies nearly parallel to the metal surface, one would expect the bending mode to be much stronger than the stretching mode. In the case of Al-Al_2O_3-Au such an intensity pattern is seen, i.e., the bending mode is seen very strongly and the stretching mode is very weak. This is suggestive of an orientation effect, but this is not conclusive and much more work will be needed to establish just what this observation means.

As has been noted, the intensity of the lines are of the order of 1% change in conductivity for a strong band. We have made no detailed study of intensity, but the order of magnitude generally observed is satisfactorily explained in terms of either mechanism which we have discussed.

B. Linewidths and Temperature Effects

It was noted that the linewidth increased with temperature, an expected result. Some of this broadening could be due to the intrinsic linewidth of the molecular vibrations, but one knows that well resolved IR and Raman spectra can be obtained even at room temperature. It is useful, therefore, to see to what extent the broadening is just the result of the electron distribution in the metals. In Fig. 15 we make a comparison of the expected line broadening with that observed at 77°K. We see that the agreement is quite reasonable. The extra width of the observed line above prediction can be accounted for by the fact that the actual linewidth as measured at 4°K was 18 mV and this will contribute to the broadening at 77°K. In fact, in a model where both broadening mechanisms are approximated by gaussian distributions, the widths of the convolution of these add as the squares. At dry ice temperature the theoretical width is about 90 mV which is in reasonable agreement with the experiment. At room temperature

the line is really too broad to make any reasonably accurate measurements, but the linewidth is certainly more than 100 mV. The predicted linewidth at room temperature is 150 mV. This of course places a severe limitation on the use of inelastic tunneling as a spectrometer at room temperature. Some useful resolution can certainly be obtained at nitrogen temperature, but helium temperatures are needed for anything where significantly detailed spectra are desired.

Measurements were made to test whether or not any significant intensity changes occurred with temperature. This means a comparison of the integrated line intensity must be made. We did not note any significant intensity change with temperature of the CH vibration line at 360 mV in agreement with the theory.

In the case of superconducting contacts one expects to achieve better resolution compared to normal metal contacts as noted in the theoretical discussion of linewidth. In addition a small shift in line position should occur (shifts of the order of the gap) and the line should also sharpen when a metal is made superconducting. The effect of magnetic fields on observed linewidth due to the quenching of a superconducting contact was examined and as expected the line was further broadened by this. Figure 16 shows the improved resolving power due to superconducting contacts. In addition, a small shift of line position, of about 1 mV to lower energy, was observed upon quenching of the superconductivity of the Pb and Al.

As regards ultimate resolution or linewidth, the experiments carried out so far cannot provide a final answer. This is because the actual observed lines are broadened by other effects in addition to the Fermi distribution broadening. This can best be illustrated by examining the sharp line in Fig. 12. This is a C≡N stretching vibration for cyanoacetic acid. We refer to it because it was one of the narrowest lines observed. At 1°K, at which point both electrodes are superconducting, this linewidth was 2 mV. This is much wider than what one would predict so that we believe this is the actual spectral linewidth. This is not at all unreasonable for solid-state spectra of course. We were unable to find any lines narrow enough to provide a test of the limiting resolution. Suffice to say that the resolution is sufficient so that one could resolve all structure usually found in IR spectra of condensed phases and in fact improve on this resolution.

The fact that the linewidths and positions behave as one would expect indicates that the initial and final states of the process do involve states near the Fermi levels in the metals at the threshold voltages. This is in agreement with what one expects for the inelastic tunneling process.

C. Range and Other Uses

In this paper we have emphasized the vibrational spectra of molecules in terms of their effects on tunneling. These effects will appear most sharply for bias voltages below 0.5 V. As indicated above, harmonics as high as 0.93 V have been observed. Thus the useful range already extends to nearly the visible part of the spectrum.

It is worthwhile to note that in discussing possible mechanisms, we essentially demonstrated a coupling to excitations via the effect on barrier. Such a coupling should exist for electron excitations as well as molecular excitations and hence it should be possible to see electronic spectra by this means. An electronic electric dipole transition, for example, would be treated in exactly the way as the molecular transition. Generally one would expect to see such effects at voltages of the order of one volt or greater although lower excitations for electronic transitions are also possible of course. It appears feasible to extend the use of this technique well into the region of visible spectra. The major problem is the breakdown strength of the insulator. The film must be about 50 Å thick and must support a field of 4×10^6 V per cm at 2 V. This begins to introduce some problems, but these are not likely to be insurmountable.

If electronic excitations can be produced one has then to consider the possibility of reradiation as light. Thus the inelastic tunneling is a potential mechanism for causing electroluminescence. In the case of molecular excitations we have assumed that the molecules relax back to their ground state by some nonradiative process, which is what one expects in solids.

In general, then, one may anticipate a variety of experiments which can be carried on involving inelastic tunneling and various excitations to which electrons can couple.

ACKNOWLEDGMENTS

The authors wish to acknowledge the very valuable technical assistance of R. M. Ager and E. B. Schermer.